Applied Catalysis B: Environmental 174–175 (2015) 486–495

Contents lists available at ScienceDirect

Applied Catalysis B: Environmental

journal homepage: www.elsevier.com/locate/apcatb

Role of trace chlorine in Ni/TiO_2 catalyst for CO selective methanation in reformate gas

Naohiro Shimoda[a], Daiki Shoji[a], Kazunori Tani[a], Masashi Fujiwara[a], Kohei Urasaki[a], Ryuji Kikuchi[b], Shigeo Satokawa[a,*]

[a] Department of Materials and Life Science, Faculty of Science and Technology, Seikei University, 3-3-1 Kichijoji-kitamachi, Musashino-shi, Tokyo 180-8633, Japan

[b] Department of Chemical System Engineering, Faculty of Engineering, The University of Tokyo, 7-3-1 Hongo, Bunkyo-ku, Tokyo 113-8656, Japan

ARTICLE INFO

Article history:
Received 3 October 2014
Received in revised form 7 February 2015
Accepted 17 March 2015
Available online 18 March 2015

Keywords:
CO selective methanation
Nickel
Titania
Chlorine component

ABSTRACT

Catalytic performance of titania supported nickel catalyst (Ni/TiO_2) with pre-treatments for the selective methanation of CO (CO-SMET) in reformate gas has been studied to elucidate the role of chlorine component in the methanation activity and CO/CO_2 reaction selectivity in CO-SMET. Raw commercial TiO_2, used as the support material, contains a certain amount of chlorine component, and the chlorine component can be removed by the heat treatment in air and water washing treatment. The Ni/TiO_2 catalyst prepared from the TiO_2 containing chlorine component exhibited high CO/CO_2 reaction selectivity, that is, low CO_2 methanation activity due to its low reverse water gas shift (r-WGS) activity, while the catalysts containing no chlorine component displayed quite low selectivity. The evaluation of the activity of the Ni/TiO_2 catalysts prepared from the starting Ni salts with different mixing molar ratios of Ni chloride and Ni nitrate indicates that a trace amount of chlorine led to the improved CO/CO_2 reaction selectivity in CO-SMET. The chlorine component in the Ni/TiO_2 catalysts is considered to be located on the interface of the Ni particles and the TiO_2 support, giving rise to the suppression of CO_2 methanation via the r-WGS step.

1. Introduction

In the hydrogen supply process to polymer electrolyte fuel cell (PEFC) systems, carbon monoxide (CO) is produced as a by-product during the reforming process of hydrocarbon fuels. The concentration of the produced CO can be lowered by water gas shift (WGS) reaction, which is still high to deteriorate the PEFC electrode performance significantly. Therefore, the deep removal of CO in the reformate gas successive to the WGS reaction is necessary for their practical usage. Preferential oxidation of CO (CO-PROX) is widely utilized for removing CO in the reformate gas after the WGS reaction [1–8]. Precious metal catalysts such as Pt [4], Rh [5], and Au [6] supported on various metal oxides and base metal catalysts such as supported Cu based catalysts [7,8] were reported to be effective for the PROX reaction. However, the PROX process requires accurate control of the air (or oxygen) injection and a fine adjustment of the reaction temperature to suppress the hydrogen oxidation as a side reaction as much as possible. Moreover, undesired dilution of the reformate gas with nitrogen occurs when air is used for this oxidation process.

Recently, CO selective methanation (CO-SMET) process represented by Eq. (1) has been considered as an effective CO removal process alternative to the CO-PROX process [9].

$$CO + 3H_2 \rightarrow CH_4 + H_2O \quad \Delta H^\circ = -206\,kJ\,mol^{-1} \tag{1}$$

Since the CO-SMET process utilizes CO and hydrogen in the reformate gas and thus does not require other additional reactants such as air in the CO-PROX process, this process can avoid the above-mentioned disadvantages of the CO-PROX process. In particular, there is no need of an air blower system specialized for the PROX reactor, which can decrease the total number of parts for the system and can result in the reduction of the manufacturing cost. In addition, the power generation efficiency would be maintained because the produced methane by CO methanation can be utilized as a fuel for steam reforming process. As a potential problem in the CO-SMET process, simultaneous methanation of the CO_2 contained in the reformate gas in a large amount (CO_2, 15–20%). The CO_2 methanation shown in Eq. (2) proceeds during CO-SMET via reverse water gas shift (r-WGS) reaction shown in Eq. (3), followed by the methanation of the produced CO by r-WGS. As a consequence, once

* Corresponding author. Tel.: +81 422 37 3757; fax: +81 422 37 3871.
E-mail address: satokawa@st.seikei.ac.jp (S. Satokawa).

http://dx.doi.org/10.1016/j.apcatb.2015.03.026
0926-3373/

the CO_2 methanation is initiated, a large amount of the hydrogen in the reformate gas is consumed. Furthermore, a thermal runaway due to the high exothermic heat of CO and CO_2 methanation is also a major concern. Therefore, a novel catalyst for CO-SMET needs to be developed, which demonstrates high activity for CO methanation and high reaction selectivity to CO methanation derived from low activity for CO_2 methanation and r-WGS.

$$CO_2 + 4H_2 \rightarrow CH_4 + 2H_2O\ \Delta H^\circ = -165\ \mathrm{kJ\,mol^{-1}} \quad (2)$$

$$CO_2 + H_2 \rightarrow CO + H_2O\ \Delta H^\circ = 41.1\ \mathrm{kJ\,mol^{-1}} \quad (3)$$

It is generally known that the group VIII transition metal catalysts exhibit high activity for CO-SMET. Especially, Ru and Ni catalysts supported on various support materials such as Ru/Al_2O_3 [10–16], Ru/zeolite [17–20], $Ru/NiAl_xO_y$ [21,22], Ru/Mesoporous-Ni-Al-O_x [23], Ru/TiO_2 [24–26], Ni/ZrO_2-SiO_2 [27], Ni/ZrO_2 [26,28], and $Ni/CaO/Al_2O_3$ [29], were reported to be effective for CO-SMET. In contrast, CO_2 methanation in the absence of CO over various supported metal catalysts was investigated by several researchers and it was reported that Ru [30–40], Rh [31,39–48], Pd [31,39,49,50], Pt [31,39], Ir [31,39], Ni [32,37,51–58], Fe [32,37], Co [32], and Ni–Fe [59,60] based catalysts are effective in CO_2 methanation. Additionally, it is generally accepted that CO_2 methanation proceeds via the r-WGS step at metal-support boundary, followed by the prompt methanation of the resultant CO [31,36,41,48]. Under the conditions of CO-SMET where CO and CO_2 coexist, it is considered that CO_2 methanation proceeds via the same mechanism and the metal-support boundary plays an important role in the r-WGS step. Indeed, Dagle *et al.* reported that the CO/CO_2 reaction selectivity of Ru/Al_2O_3 is strongly affected by the ruthenium particle size, and that the Ru/Al_2O_3 with smaller ruthenium particles exhibits the lower CO/CO_2 selectivity [14]. A good correlation of the CO_2 methanation rate in CO-SMET with the perimeter length of Ru particles on Ru/TiO_2 and Ru/Al_2O_3 catalysts was reported by Tada *et al.* [61], which also supports the interface between the active species and the support is the reaction site for CO_2 methanation via the r-WGS reaction.

In our recent work, we have reported that Ru and Ni based catalysts exhibited superior activity [61–68] for CO-SMET. Especially, Ru and Ni catalysts supported on the titania supplied from Evonik Degussa (P25) showed high activity for CO methanation with high CO/CO_2 reaction selectivity in the CO-SMET reaction. Moreover, we have revealed that the formation of CO via r-WGS was suppressed even at high reaction temperatures over Ni/TiO_2. As a result, "temperature window", where CO is removed sufficiently without significant methane formation, of Ni/TiO_2 was much larger than that of Ni/Al_2O_3 [63]. In addition, the effect of starting materials of Ni species has been studied on the performance of Ni/TiO_2 for CO-SMET. Consequently, we have revealed that the Ni/TiO_2 prepared from Ni nitrates exhibited high activity and high selectivity, but the one prepared from Ni chlorides exhibited much higher reaction selectivity of CO/CO_2 although its activity of CO methanation was slightly inferior [64].

Djinović *et al.* studied the effect of the chlorine addition to Ru/Al_2O_3 catalyst and reported the improvement of the CO/CO_2 selectivity due to the inhibition of hydrogenation of CO_2 [10,69]. In addition, Miyao and Higashiyama *et al.* have investigated the effect of Ru chloride addition to the Ni-Al oxides catalyst prepared by the spray pyrolysis method. They have performed catalytic activity tests and Fourier transform infrared spectroscopy (FT-IR) analysis, and have revealed the positive effect of the chloride addition to Ni–Al oxides on the CO/CO_2 selectivity in CO-SMET [21–23]. In addition, Zyryanova *et al.* have studied the effect of large amount of chlorine loading on the performance of the ceria supported Ni catalyst for CO-SMET and have suggested that the chlorine species present at the ceria surface result in high CO/CO_2 selectivity possibly because the catalytic activity for the methanation of CO and CO_2 is modified in a different manner by the presence of the chlorine species [70].

Based on these studies in the CO-SMET over several catalysts, it is worth noting that chlorine component remaining in the catalyst affects the catalytic performance, especially, the CO/CO_2 reaction selectivity. It is known that a trace amount of chlorine resides in the TiO_2 (P25) used as a support material in our previous works. Therefore, in the present study, we have focused on the effect of chlorine content in Ni/TiO_2 on the catalytic activity and the reaction selectivity for CO-SMET. Several treatments for the TiO_2 support and prepared Ni/TiO_2 catalysts have been conducted and various starting materials of the Ni component have been employed in the preparation procedure of Ni/TiO_2 catalysts, to investigate systematically the effect of the residing chlorine species on the activity and selectivity of CO/CO_2 methanation in CO-SMET and to attain further scientific insights into the role of the chlorine component in CO-SMET.

2. Experimental

2.1. Catalyst preparation

All the Ni/TiO_2 catalysts were prepared by the impregnation method from an aqueous solution of nickel(II) chloride hexahydrate ($NiCl_2{\cdot}6H_2O$, Wako Pure Chemical Ind.) and nickel(II) nitrate hexahydrate ($Ni(NO_3)_2{\cdot}6H_2O$, Kanto Chemical Co.) mixture with an appropriate molar ratio. Details are referred to in our previous report [62,64]. As a support, commercial TiO_2 (Evonik Degussa, P25) was used in the present study. To remove the chlorine component, pre-treatments of TiO_2 were carried out as follows: heat treatment in air for 2 h at 500 °C and 800 °C (abbreviated to TiO_2-500 and TiO_2-800, respectively); repetitive water washing at 50 °C for 1 h (abbreviated to TiO_2-water). The Ni content for all the prepared catalysts was adjusted to 10 wt% in its metallic state. The obtained samples were calcined in air at 500 °C for 2 h and then pressed, crushed, and sieved to particle size of 150–250 μm for the catalytic activity tests of CO-SMET. Hereafter, the prepared catalysts were abbreviated as "Ni(*x*:*y*)/TiO_2-*T*" in which *x*:*y* represents the molar ratio of Ni chloride to Ni nitrate and *T* denotes the heat treatment temperature of the TiO_2 support, as mentioned above. The support used without the heat treatment is denoted as TiO_2-as.

2.2. Catalytic activity and durability evaluation

Catalytic activity tests of CO-SMET were carried out in a fixed bed flow reactor at 150–300 °C under atmospheric pressure. The Ni(*x*:*y*)/TiO_2-*T* catalyst of 300 mg was set in the reactor and then reduced in 20% H_2/N_2 at 450 °C for 30 min prior to the activity test. A reaction gas mixture (0.2% CO, 16.4% CO_2, 64.8% H_2, and 18.6% H_2O), which simulates the outlet gas of the WGS converter equilibrated at 180 °C derived from an initial steam carbon ratio (S/C) = 3, was fed to the catalyst bed at a desired ratio of weight of catalyst to flow rate of CO (W/F_{-CO}). After water vapor was segregated in an ice-water trap from the reaction gas mixture, the dry gaseous compositions of the influent and effluent gases were analyzed using a gas chromatograph equipped with a thermal conductivity detector (Shimadzu, GC-8A). A SHINCARBON ST 50–80 column (Shinwa Chem. Ind.) was used for the separation of CO, CO_2, and H_2.

2.3. Catalyst characterization

To identify the crystalline structures, the powder X-ray diffraction (XRD) patterns were obtained in air using a Rigaku Ultima IV, equipped with Cu Kα radiation source (λ = 0.154 nm). The typical working conditions such as an acceleration voltage and current

were 40 kV and 40 mA with a scanning speed of 1° min^{-1}. The crystallite size of Ni (111) was calculated by the XRD-line broadening analysis using Scherrer's equation as follows:

$$D = \frac{K\lambda}{\beta \cos\theta} \quad (4)$$

where K is the shape factor (0.89), λ is X-ray wavelength (0.154 nm), β is the line broadening at half the maximum intensity in radians, and θ is Bragg angle.

The specific surface area of each TiO_2 with several pre-treatments was determined by N_2 adsorption measurements at 77 K with the conventional BET method using a BEL Japan BELSORP-mini II instrument. Prior to N_2 adsorption, each sample was out-gassed at 300 °C for 0.5 h in order to remove the moisture adsorbed on the surface and inside the porous network.

Transmission electron microscopy (TEM) analysis of several TiO_2 supported Ni catalysts was performed using a JEOL JEM-2100F operated at 200 kV. The samples were dispersed by ultrasonic in acetone followed by deposition of the suspension onto a standard Cu grid covered with a holey carbon film.

To estimate the amount of the residual chlorine in the catalysts, the supernatant liquid after the water washing was analyzed using an ion chromatography (IC, Shimadzu, CDD-6A) equipped with a Shim-pack IC-C3 column (Shimadzu GLC). Deionized water was added to the sample by a ratio of 100 mL g-cat^{-1}. The specimen was stirred for a day and then filtered to separate the catalyst from the wash liquid. This supernatant liquid was analyzed by IC to measure the amount of chlorine. The obtained specimen was dried in air at 110 °C for 1 h. The water washing treatment was repeated until no chlorine content was detected by the IC analysis. Here, we note that the lower detection limit of chlorine by the IC analysis was 1.1 ppm-wt. in the present study.

To study the decomposition behavior of the catalysts, thermogravimetry (TG) and differential thermal analysis (DTA) were conducted using a Rigaku Thermoplus TG 8120. The TG-DTA measurement was carried out under air atmosphere at heating rate of 10 °C min^{-1} from room temperature to 900 °C. The Ni(10:0)/TiO_2-500 and Ni(0:10)/TiO_2-500 catalysts after the calcination in air at 500 °C for 2 h, and the as-obtained Ni chloride hexahydrate and nitrate hexahydrate samples (*ca.* 40 mg) were used for TG-DTA measurement.

To elucidate the adsorbed species and intermediates during CO_2 methanation over several TiO_2 supported Ni catalysts, FT-IR measurements were conducted using a JASCO FT/IR-4100 equipped with a glass reaction cell (Makuhari Rikagaku Garasu Inc.). The catalyst thin disks were made and placed in the FT-IR cell. The spectra were recorded in Ar at 150 °C on the Ni(0:10)/TiO_2-500, Ni(0:10)/TiO_2-water, and Ni(0:10)/TiO_2-as catalysts after the pre-treatments as follows: firstly reduced in 20% H_2/Ar at 450 °C for 1 h, and then CO_2 was adsorbed at 150 °C for 30 min, and subsequently purged with Ar for 80 min, followed by the reaction in 20% H_2/Ar for 1 h. Back ground spectra were recorded in Ar at 150 °C prior to the CO_2 adsorption step. The measurement was operated at a scan speed of 50 scan per minute and a resolution of 4 cm^{-1}, and 240 scans were collected for each spectrum.

3. Results and discussion

3.1. Effect of pre-treatment of titania

Fig. 1 shows the results of the catalytic activity test for CO-SMET over the Ni/TiO_2 catalysts prepared from only Ni nitrate and the TiO_2 supports with and without pre-treatments. For the Ni catalyst supported on the as-obtained TiO_2 (Ni(0:10)/TiO_2-as, □), the CO concentration in the effluent gas was maintained at low level and the abrupt increase in the CH_4 concentration was

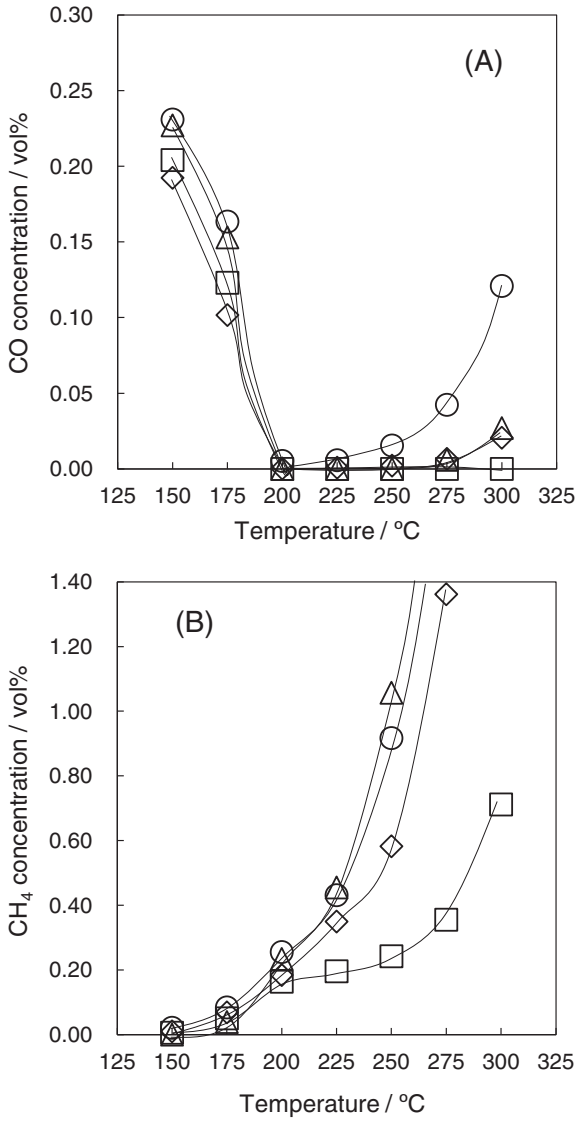

Fig. 1. (A) CO concentration and (B) CH_4 concentration for CO-SMET over (○) Ni/TiO_2-800, (◊) Ni/TiO_2-500, (△) Ni/TiO_2-water, and (□) Ni/TiO_2-as. Reaction condition: 0.2% CO, 16.4% CO_2, 64.8% H_2, 18.6% H_2O; $W/F_{\cdot CO}$ = 0.7 kg h mol^{-1}.

suppressed even at the high temperatures above 250 °C. Consequently, a plateau appeared in the CH_4 concentration profile, which indicates that the initiation of CO_2 methanation is decelerated over Ni(0:10)/TiO_2-as. In addition, the CH_4 concentration at the plateau was *ca.* 0.25% and corresponds to the value for which almost all CO in the influent gas is converted to CH_4. As the CO concentration was almost zero in the temperature range where the plateau appeared, it can be considered that almost no CO_2 is converted to CH_4 in the temperature range. According to Henderson and Worley [42], CO_2 methanation is inhibited by trace amount of CO, and consequently CO_2 methanation can proceed forward after the consumption of CO by methanation. Therefore, the appearance of such a plateau in the CH_4 concentration profile indicates an excellent performance in CO/CO_2 methanation selectivity. In contrast, for the pre-treated TiO_2 supported Ni catalysts with the washing treatment (Ni(0:10)/TiO_2-water, △) and the heat treatment at 500 °C (Ni(0:10)/TiO_2-500, ◊) and 800 °C (Ni(0:10)/TiO_2-800, ○), the CH_4 concentration increased continuously as the reaction temperature was raised, with a slight gradient change in the curve above the CH_4 concentration of *ca.* 0.25%. This trend indicates that CO_2 methanation promptly proceeds over these pre-treated catalysts, and it can

Table 1
Structural properties of the TiO_2 without and with pre-treatments and the spent Ni(0:10)/TiO_2 catalysts after the CO-SMET shown in Fig. 2.

Pre-treatment	BET S.A. of TiO_2 ($m^2\ g^{-1}$)	Crystalline phase of TiO_2	Crystallite size of metallic Ni (1 1 1) (nm)
Heat treatment at 800 °C	14	Rutile	24.1
Heat treatment at 500 °C	58	Anatase[a], Rutile	18.9
Water washing	58	Anatase[a], Rutile	12.3
As-obtained	59	Anatase[a], Rutile	12.6

[a] Anatase phase mainly was observed.

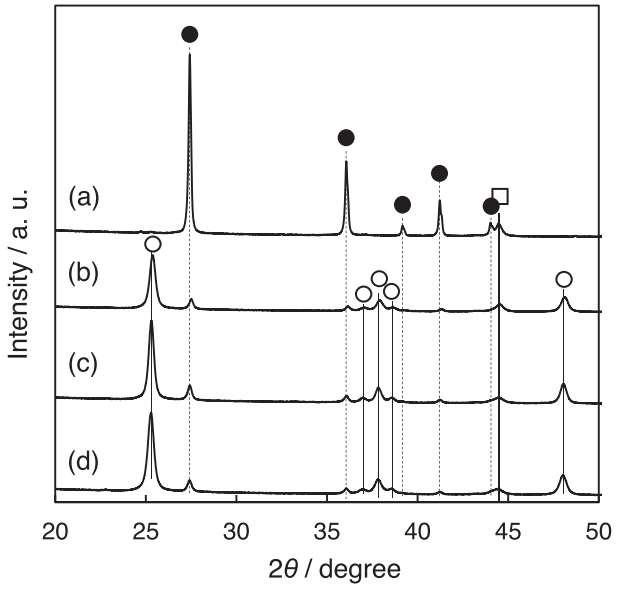

Fig. 2. XRD patterns of the spent Ni/TiO_2 catalysts after the CO-SMET shown in Fig. 1: (a) Ni/TiO_2-800, (b) Ni/TiO_2-500, (c) Ni/TiO_2-water, (d) Ni/TiO_2-as. Symbol: (◯) TiO_2 (Anatase), (●) TiO_2 (Rutile), (□) Ni metal.

be concluded that the CO/CO_2 selectivity over the pre-treated TiO_2 supported Ni catalysts is degraded. As for the CO concentration, it increased drastically above 250 °C, especially over Ni(0:10)/TiO_2-800 (◯). The CO concentration can be determined by the balance between CO consumption by the CO methanation reaction and CO formation by the r-WGS reaction. Consequently, the highest CO concentration over Ni(0:10)/TiO_2-800 implies that Ni(0:10)/TiO_2-800 is inferior to the other pre-treated catalysts concerning CO methanation activity. The progression of r-WGS in the high temperature region results in the increase in CO concentration as well as the conversion of CO_2, and consequently is unfavorable for CO-SMET.

To elucidate the effect of the above-mentioned pre-treatments, several characterizations were conducted. Fig. 2 represents the XRD patterns of the spent Ni/TiO_2 catalysts after the activity tests of CO-SMET shown in Fig. 1. There was no apparent difference among the Ni(0:10)/TiO_2-water, Ni(0:10)/TiO_2-500, and Ni(0:10)/TiO_2-as catalysts: Anatase phase was mainly observed and rutile phase was also recognized slightly. By contrast, the main crystalline structure of the TiO_2 was changed from anatase to rutile phase for the Ni(0:10)/TiO_2-800 catalyst.

The BET surface areas and crystalline phases of pure TiO_2 supports without and with pre-treatments, and crystallite sizes of metallic Ni (1 1 1) of the spent catalysts are summarized in Table 1. The surface areas of the TiO_2 with the heat treatment in air at 500 °C and the water washing were almost same with that of the TiO_2 as obtained (58–59 $m^2\ g^{-1}$). In contrast, the surface area of the TiO_2 after the heat treatment in air at 800 °C decreased significantly (from 59 $m^2\ g^{-1}$ to 14 $m^2\ g^{-1}$).

TEM images of the spent catalysts are shown in Fig. 3. As can be seen in Fig. 3a, the TiO_2 particles in Ni(0:10)/TiO_2-800 were larger than those in the others, and furthermore, the large Ni particles were observed. This indicates that the heat treatment of TiO_2 at 800 °C leads to the significant transition of catalyst structure, as confirmed by the XRD and BET surface area analyses.

As summarized in Table 1, the crystallite sizes of metallic Ni (1 1 1) plane in the spent Ni(0:10)/TiO_2-800 and Ni(0:10)/TiO_2-500 catalysts were 24.1 nm and 18.9 nm, respectively. Whereas, the ones of the spent Ni(0:10)/TiO_2-water and Ni(0:10)/TiO_2-as catalysts were below 13 nm. The Ni particles observed in TEM analysis for the spent Ni(0:10)/TiO_2-water and Ni(0:10)/TiO_2-as catalysts were smaller than those of Ni(0:10)/TiO_2-800. However, there was no significant difference in the catalyst structure between the Ni(0:10)/TiO_2-water and Ni(0:10)/TiO_2-as catalysts, even though it seems that Ni particles of the Ni(0:10)/TiO_2-500 catalyst agglomerated slightly.

These results indicate that there is no apparent correlation among the crystalline phase and surface area of TiO_2, the crystallite size of metallic Ni in the catalysts, and the catalytic performance of the Ni/TiO_2 catalysts for CO-SMET. Thus, we have focused on the effect of chlorine content in Ni/TiO_2, as another factor by the water washing treatment and the heat treatment in air at 500 °C, on the reactivity of Ni/TiO_2 catalyst for CO-SMET.

The amount of residual chlorine in TiO_2 (P25) was measured by the IC analysis. As shown in Table 2, we found that chlorine component in the as-obtained TiO_2 can be removed by more than three times of the water washing treatment to the low concentration level which is lower than the detection limit of the IC analysis (1.1 ppm-wt.). The calculated total amount of chlorine content in the as-obtained TiO_2 was *ca.* 1500 ppm-wt. Meanwhile, no chlorine content was detected for the supernatant wash liquid of the TiO_2-500 and TiO_2-800, indicating that the heat treatments in air at 500 °C and 800 °C can also remove the chlorine contained in the as-obtained TiO_2 adequately. During the CO-SMET reaction shown in Fig. 1B, CH_4 formation was suppressed over the only Ni(0:10)/TiO_2-as catalyst, leading to high CO/CO_2 reaction selectivity. Therefore, we consider that the residual chlorine content in Ni/TiO_2 catalysts certainly has a positive effect on the reaction selectivity in CO-SMET.

3.2. *Effect of chlorine content in Ni/TiO_2 catalyst*

In the study of CO-SMET reaction, some researchers have reported the chlorine effect; Djinović [69], Miyao [21,22], and

Table 2
Residual chlorine content in TiO_2 (P25) after the water washing treatment.

Washing number of times	Residual chlorine (ppm-wt.)
1st	929
2nd	420
3rd	135
4th	n.d.[a]
5th	n.d.[a]
Total	1484

[a] n.d.: under the detection limit of ion chromatography analysis (1.1 ppm-wt.).

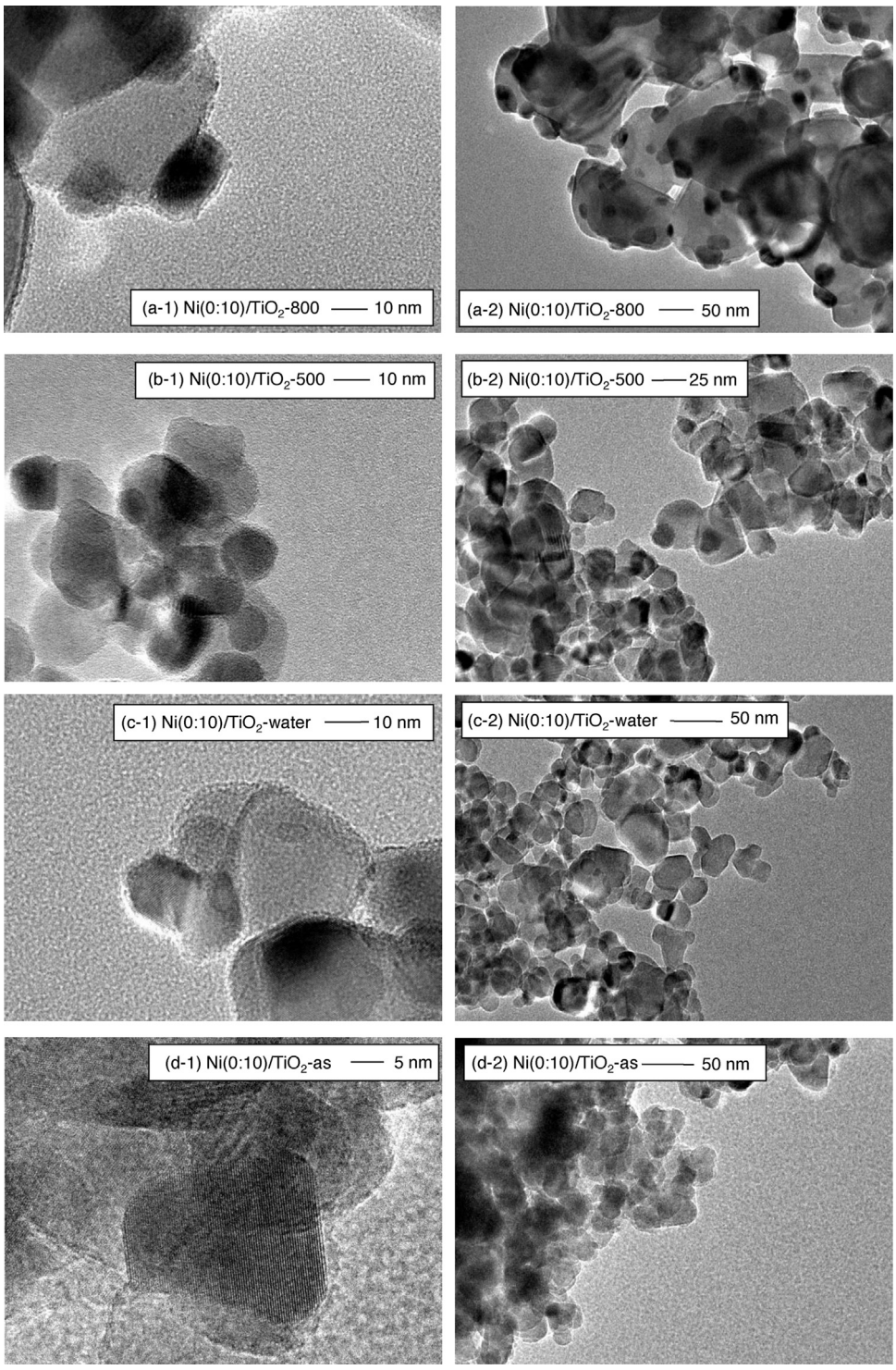

Fig. 3. TEM images of the spent Ni/TiO_2 catalysts after the CO-SMET shown in Fig. 1: (a) Ni/TiO_2-800, (b) Ni/TiO_2-500, (c) Ni/TiO_2-water, (d) Ni/TiO_2-as.

Zyryanove [70] *et al.* have studied on the chlorine effect over Ru/Al_2O_3 and Ni/Al_2O_3 catalysts as mentioned in the Introduction section. Thus, in the present study, we have studied the additional effect of chlorine content over Ni/TiO_2 catalyst. The effect of mixing molar ratio of the starting Ni salts on the catalytic reactivity for CO-SMET was investigated using the Ni catalysts supported on the TiO_2-500 that contains no chlorine component. We suppose that the chlorine component residing on the Ni/TiO_2 catalysts increases consistently with the chloride content in the starting mixture of the Ni salts. As shown in Fig. 4, Ni(1:9)/TiO_2-500 (◊) decreased CO concentration rapidly comparable to Ni(0:10)/TiO_2-500 (□), and the further increase in the chlorine content resulted in the degradation of the CO removal ability. Nevertheless, the CO concentration over Ni(2:8)/TiO_2-500 (△) was decreased to approximately 0 vol% at 200 °C, which is comparable to Ni(1:9)/TiO_2-500 and Ni(0:10)/TiO_2-500. The CO concentration over the chlorine-containing catalysts were maintained at quite low concentration even above 250 °C, whereas a slight increasing trend in the CO concentration was observed for Ni(0:10)/TiO_2-500. As for the amount of CH_4 formation, the most rapid increase in the CH_4

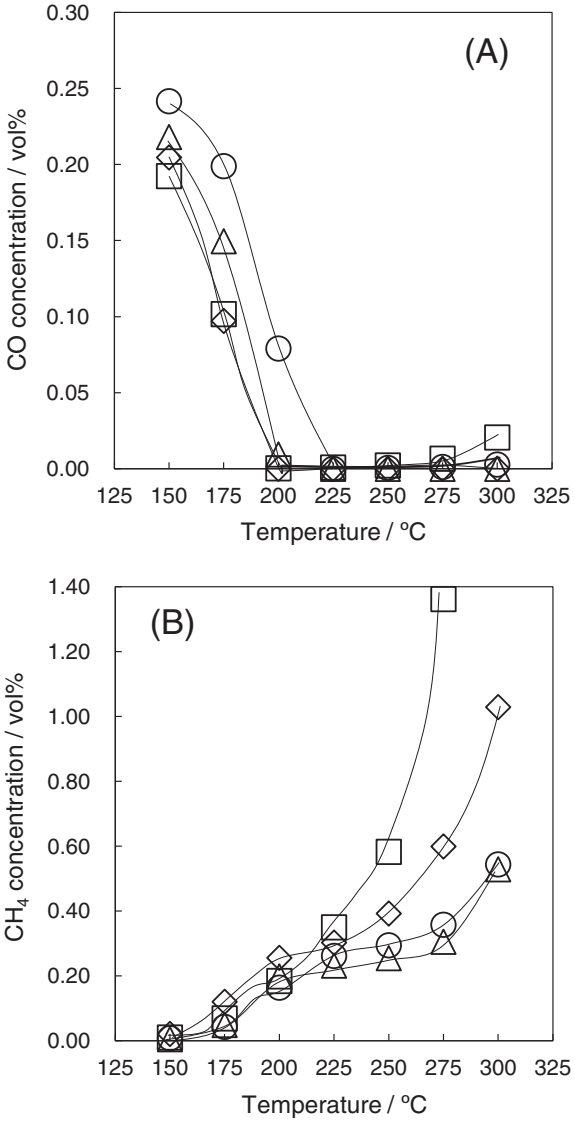

Fig. 4. (A) CO concentration and (B) CH_4 concentration for CO-SMET over Ni(*x*:*y*)/TiO_2-500 catalysts: (□) Ni(0:10)/TiO_2-500, (◊) Ni(1:9)/TiO_2-500, (△) Ni(2:8)/TiO_2-500, (○) Ni(10:0)/TiO_2-500. (*x*:*y*): mixing molar ratio of Ni chloride to Ni nitrate. Reaction condition: 0.2% CO, 16.4% CO_2, 64.8% H_2, 18.6% H_2O; $W/F_{\cdot CO} = 0.7$ kg h mol^{-1}.

concentration was observed over Ni(0:10)/TiO_2-500 (□), followed by Ni(1:9)/TiO_2-500 (◊). The CH_4 concentration was slightly higher over Ni(1:9)/TiO_2-500 than Ni(0:10)/TiO_2-500 up to the temperature of 200 °C and the CH_4 concentration of *ca.* 0.25 vol%, which agrees well with the CO concentration profiles in Fig. 4A and confirms CO methanation proceeds preferentially in this region.

Above this temperature, the CH_4 concentration increased more steeply over Ni(0:10)/TiO_2-500 (□) than Ni(1:9)/TiO_2-500 (◊). This result indicates that the Ni catalyst with chlorine component suppresses CO_2 methanation more effectively than the one without. The increase in the chlorine content further inhibited CO_2 methanation, that is, the amount of CH_4 formed over the Ni(10:0)/TiO_2-500 (○) prepared from only Ni chloride was as small as that over Ni(2:8)/TiO_2-500 (△). In spite of the low CO_2 methanation activity, the CO concentration at 200 °C over the Ni(10:0)/TiO_2-500 was *ca.* 0.08 vol% and larger than those over the other catalysts. These results indicate that the chlorine component lowers the CO methanation activity slightly, but more effectively suppresses CO_2 methanation activity, leading to the improved CO/CO_2 reaction selectivity in CO-SMET.

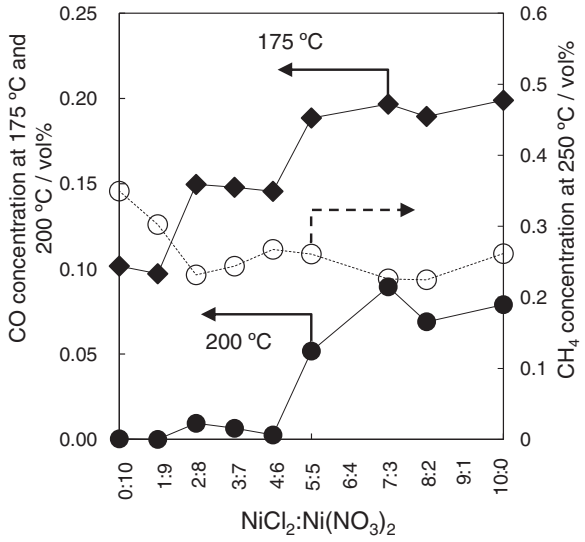

Fig. 5. Effect of mixing molar ratio of Ni chloride to Ni nitrate on CO concentration at (●) 200 °C and (♦) 175 °C, and (○) CH_4 concentration at 250 °C for CO-SMET over Ni/TiO_2-500 catalysts. (*x*:*y*): mixing molar ratio of Ni chloride to Ni nitrate. Reaction condition: 0.2% CO, 16.4% CO_2, 64.8% H_2, 18.6% H_2O; $W/F_{\cdot CO} = 0.7$ kg h mol^{-1}.

Furthermore, several Ni/TiO_2-500 catalysts were prepared from Ni salt solutions with different mixing molar ratios of Ni chloride to Ni nitrate, and their catalytic performance was evaluated. In Fig. 5, the CO concentrations at 175 °C and 200 °C and the CH_4 concentration at 250 °C in the effluent gas reacted over the Ni(*x*:*y*)/TiO_2-500 catalysts are plotted for the molar ratios of Ni chloride to Ni nitrate, *x*:*y*. The CO concentrations at 175 °C and 200 °C increased gradually with an increase in the molar ratio of Ni chloride to Ni nitrate, indicating the degradation of the catalytic activity of Ni/TiO_2 for CO methanation. In contrast, the CH_4 formation at 250 °C decreased from 0.35 vol% to 0.23 vol% with the chlorine addition at molar ratio of 2:8, and the further addition of chlorine content had no significant effect on the amount of the CH_4 formation. Therefore, we conclude that the addition of a trace amount of chlorine component is effective for the catalytic performance of Ni/TiO_2 for CO-SMET. It should be noted that carbon deposition in CO-SMET was not evoked by the chlorine component addition, which we confirmed by temperature programmed oxidation (TPO) analysis of the spent catalysts and the carbon balance of the influent and effluent gases.

Fig. 6 shows the XRD patterns of the spent Ni(*x*:*y*)/TiO_2-500 catalysts after the activity test of CO-SMET shown in Figs. 4 and 5. The diffraction intensity of each sample was normalized using the peak of TiO_2 (1 0 1) plane. The crystallite sizes of metallic Ni (1 1 1) plane in the spent Ni(*x*:*y*)/TiO_2-500 catalysts are summarized in Table 3. After the activity test, anatase and rutile phases of TiO_2 and metal-

Table 3
Crystallite size of metallic Ni (111) in the spent[a] Ni(*x*:*y*)/TiO_2-500 catalysts.

Molar ratio of $NiCl_2$ to Ni $(NO_3)_2$	Crystallite size of Ni (nm)
10:0	42.2
8:2	37.8
7:3	38.0
5:5	27.8
4:6	26.1
3:7	26.2
2:8	24.9
1:9	18.6
0:10	18.9

[a] After the CO-SMET activity test shown in Figs. 4 and 5.

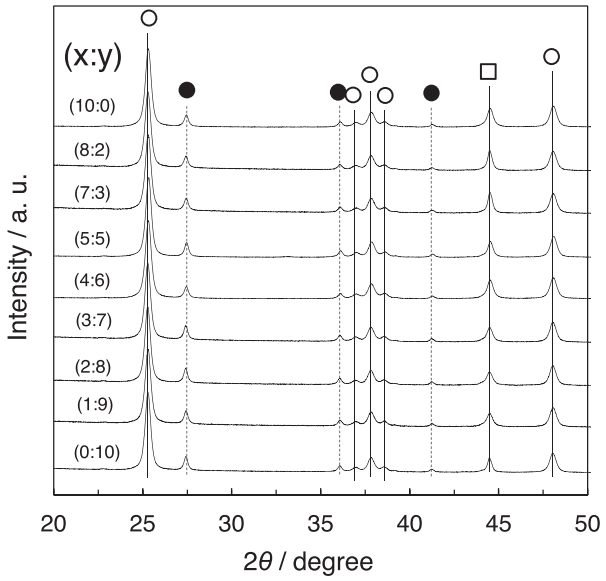

Fig. 6. XRD patterns of the spent Ni(*x*:*y*)/TiO_2-500 catalysts after the CO-SMET shown in Figs. 4 and 5. Symbol: (○) TiO_2 (Anatase), (●) TiO_2 (Rutile), (□) Ni metal.

lic Ni phase were observed in all the spent catalysts, giving close agreement with the results of the spent Ni(0:10)/TiO_2-500, -water, and -as catalysts shown in Fig. 2. The crystallite size of metallic Ni increased with an increase in the molar ratio of Ni chloride to Ni nitrate. From these results, we consider that the decrease in the catalytic activity for CO methanation with an increase in the molar ratio of Ni chloride is possibly due to Ni particle size growth indicated by the crystallite size growth of metallic Ni, which leads to a decrease in the number of the active sites. The IC analysis revealed that *ca.* 940 ppm-wt. of chlorine remained in the spent Ni(10:0)/TiO_2-500 catalyst prepared from only Ni chloride, and that no chlorine content was detected for the spent Ni(0:10)/TiO_2-500 catalyst which were free from chlorine component in the preparation procedure. On the other hand, for the catalysts prepared from several mixtures of Ni chloride and Ni nitrate, no clear correlation was found between the catalytic performance and the amount of residual chlorine (results are not shown).

As shown in Fig. 7a and b, the TG-DTA measurement in air was conducted for the Ni(10:0)/TiO_2-500 and Ni(0:10)/TiO_2-500 catalysts after the calcination in air at 500 °C. The weight decrease and endothermic peak attributed to the dehydration of the adsorbed water on the catalyst appeared below 150 °C for both samples. The weight of the Ni(10:0)/TiO_2-500 catalyst (a) prepared from only Ni chloride decreased drastically at *ca.* 500 °C, which can be ascribed to the oxidative decomposition of Ni chloride to Ni oxide. In contrast, for the Ni(0:10)/TiO_2-500 catalyst (b), the weight decrease

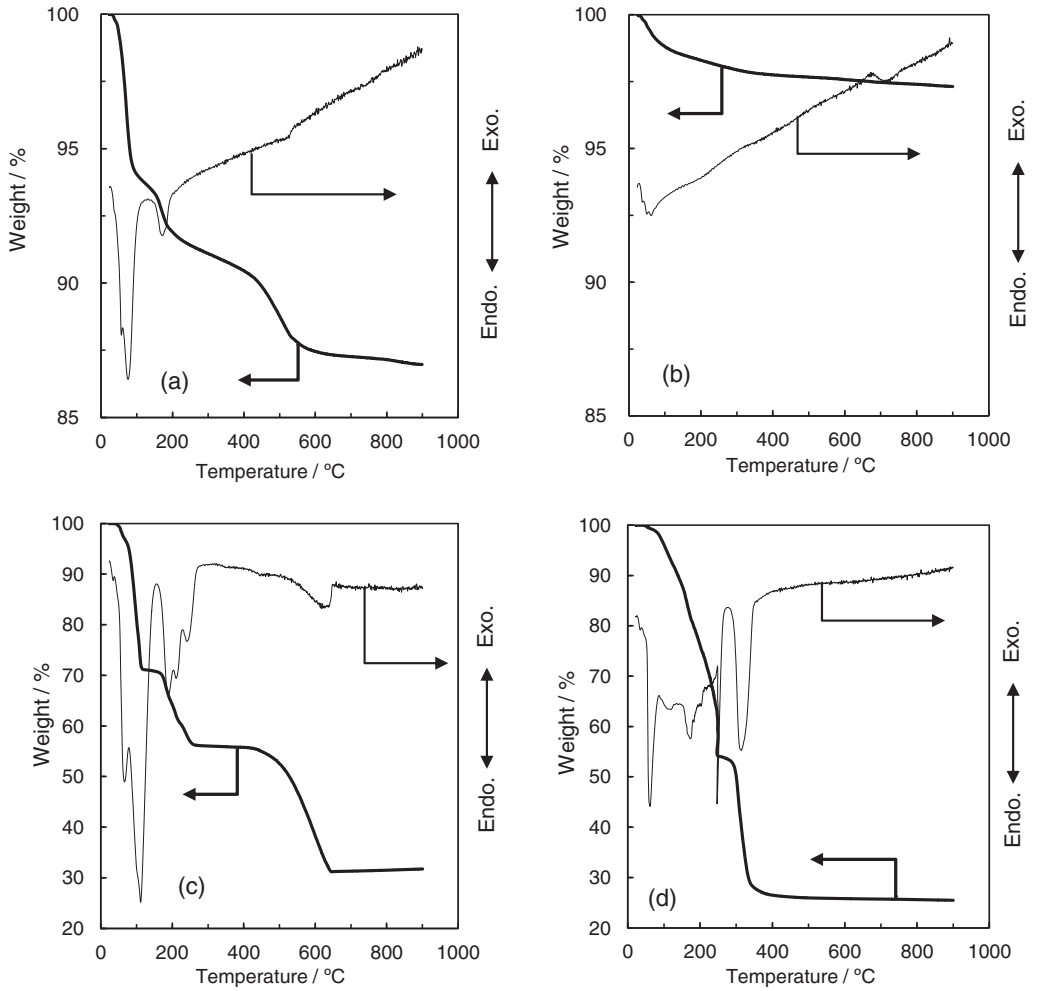

Fig. 7. TG-DTA profiles of (a) Ni(10:0)/TiO_2-500 and (b) Ni(0:10)/TiO_2-500 after the calcination in air at 500 °C, and the as-obtained (c) Ni chloride hexahydrate and (d) Ni nitrate hexahydrate.

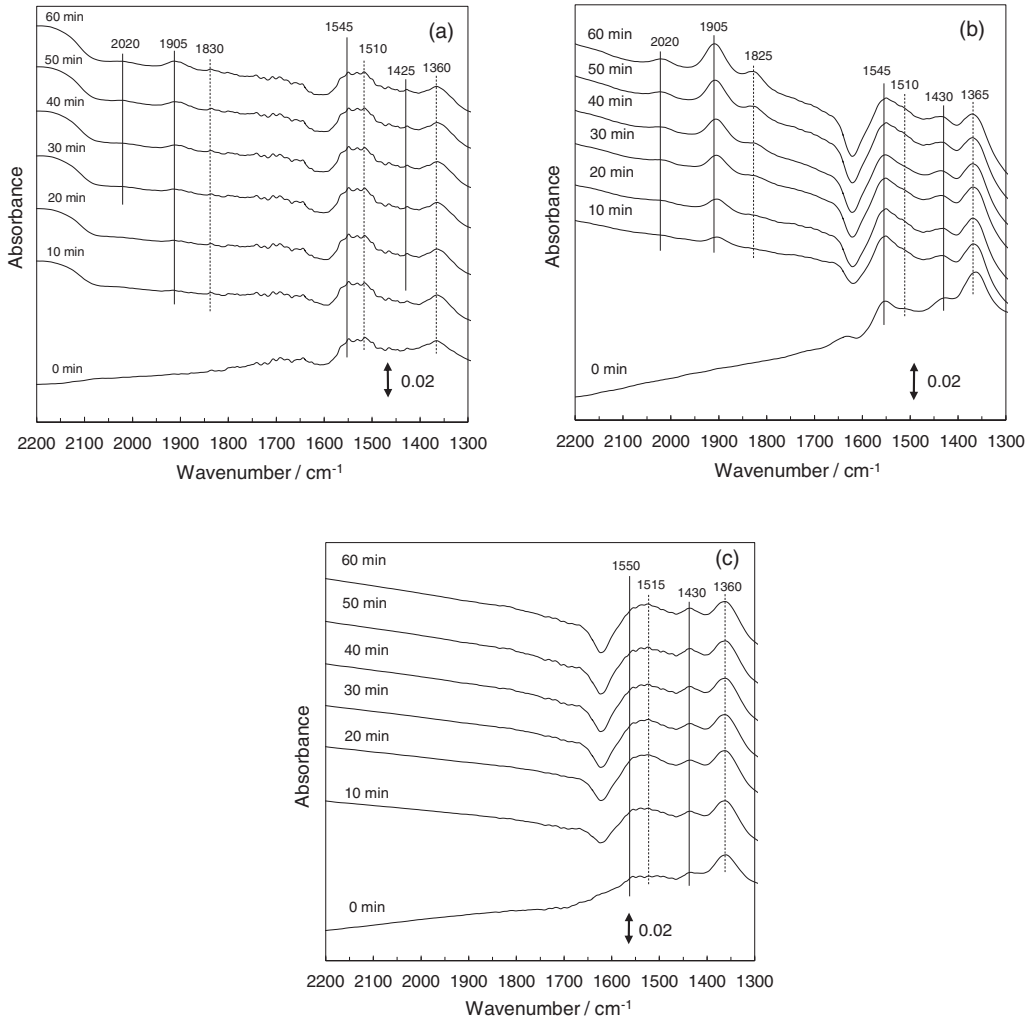

Fig. 8. FT-IR spectra on the Ni/TiO_2 catalysts during CO_2 methanation: (a) Ni(0:10)/TiO_2-500, (b) Ni(0:10)/TiO_2-water, (c) Ni(0:10)/TiO_2-as. These spectra were recorded in Ar at 150 °C after the pre-treatment as follows: first reduced in 20% H_2/Ar at 450 °C for 1 h, and then CO_2 was adsorbed at 150 °C for 30 min, and subsequently purged with Ar at 150 °C for 80 min, followed by reaction in 20% H_2/Ar at 150 °C for 60 min. Back ground spectra were recorded in Ar before the CO_2 adsorption step at 150 °C.

stemming from possible decomposition of Ni nitrate was quite small, indicating that Ni nitrate is decomposed to Ni oxide by the final calcination in the catalyst preparation. This is evidenced by the TG-DTA analysis of Ni chloride hexahydrate and Ni nitrate hexahydrate samples shown in Fig. 7c and d that the Ni nitrate was decomposed completely until 400 °C, whereas the Ni chloride decomposition was completed above 600 °C. These results indicate that not all Ni chloride is decomposed during the calcination at 500 °C in the catalyst preparation process and remained in the Ni(10:0)/TiO_2-500 catalyst prepared from only Ni chloride even after the calcination process.

Although the chlorine component contained in the as-obtained TiO_2 can be removed completely by the heat treatment at 500 °C in air as shown in Table 2, the chlorine component resides on the Ni(10:0)/TiO_2-500 catalyst even after the same heat treatment at 500 °C in air, as demonstrated by the TG-DTA analysis shown in Fig. 7. It is of note that by the IC analysis *ca.* 250 ppm-wt. of chlorine component was detected in the Ni(0:10)/TiO_2-as catalyst that was prepared from only Ni nitrate and the as-obtained TiO_2 support. This is probably because Ni chloride species can be formed by the interaction of the Ni species from the nitrate with the chlorine component residing in the as-obtained TiO_2. Once such Ni chloride species are formed, they are not completely decomposed to Ni oxide by the heat treatment at 500 °C in air during the catalyst preparation. Accordingly, it is assumed that such Ni chloride species can be formed in the vicinity of the Ni species and reside at the interface of the Ni and TiO_2. The formation of such Ni chloride at the interface is essential in inhibiting CO_2 conversion to intermediates in r-WGS such as formate species [53,61,65]. Furthermore, since the CO methanation activity was maintained as shown in Fig. 4, the active sites at the Ni surface should be free from the Ni chloride species. These assumptions are supported by the results that Ni(0:10)/TiO_2-as suppressed the conversion of CO_2 to CO via r-WGS with the CO methanation activity maintained, and that Ni(0:10)/TiO_2-500 which is free from chlorine component accelerated the CO_2 conversion to CH_4, as shown in Fig. 1.

Fig. 8 shows FT-IR spectra on the Ni(0:10)/TiO_2-500, Ni(0:10)/TiO_2-water, and Ni(0:10)/TiO_2-as catalysts during CO_2 methanation at 150 °C. Immediately after switching the atmosphere from H_2/Ar to Ar, for all catalysts, several bands appeared at approximately 1510 and 1360 cm^{-1}, and 1545 and 1430 cm^{-1}, assignable to formate species and bicarbonate species, respectively [4,35]. These intermediates are considered to be formed by the adsorption of CO_2 on the TiO_2 surface. The bands at approximately 2020 and 1900 cm^{-1}, and 1820 cm^{-1} gradually grew with the elapse of time for the Ni(0:10)/TiO_2-water catalyst. These can be assigned to linear CO and bridge CO, respectively [4,21,35]. For the Ni(0:10)/TiO_2-500 catalyst, the formation of CO adsorbed species

was observed after 40 min, while there were no bands attributed to the CO species over the Ni(0:10)/TiO_2-as catalyst. These results gave the evidence of the positive effect of chlorine component on selective CO methanation, that is, the inhibition effect on CO_2 conversion to CO by r-WGS. It can be, therefore, concluded that the trace amount of chloride component in the Ni(0:10)/TiO_2-as catalyst is effective in suppressing the decomposition of the intermediates such as bicarbonate and formate species to form CO.

As the effect of the residual chlorine in Ni/TiO_2 catalysts, retarding the CO_2 methanation can be considered at the high temperature region above 200 °C. Consequently, the addition of chlorine content reduces the CH_4 formation derived from CO_2, leading to the improvement of CO/CO_2 reaction selectivity of the Ni/TiO_2 catalysts. However, the excess addition of chlorine component facilitates the crystal growth of Ni species, resulting in a decrease of the catalytic activity for CO methanation due to a decrease in the number of the active sites. Thus, we conclude that among the catalysts evaluated in the present study, the Ni(2:8)/TiO_2-500 catalyst is an optimal catalyst, which exhibits high activity for CO methanation and superior CO/CO_2 reaction selectivity in CO-SMET, in comparison to the Ni(0:10)/TiO_2-as catalyst.

4. Conclusions

The effect of chlorine content in the Ni/TiO_2 catalysts on the catalytic performance for CO-SMET in reformate gas has been studied. The experimental findings and conclusive remarks in the present study are summarized as follows:

- Raw commercial TiO_2, used as the support material, contains a certain amount of chlorine component. The chlorine component in the TiO_2 can be removed by the heat treatment in air at 500 °C and 800 °C and the water washing treatment. When the chlorine component was removed from TiO_2 and the treated TiO_2 supports were used for Ni/TiO_2 catalysts, the conversion of CO_2 to CO was enhanced in comparison with the Ni/TiO_2 without the pre-treatments. The resultant CO was promptly converted to CH_4 and consequently the CH_4 concentration increased steeply. It can be concluded that the Ni/TiO_2 catalyst prepared from the TiO_2 containing a trace amount of chlorine exhibits high CO methanation activity and high CO/CO_2 reaction selectivity, that is, low CO_2 methanation activity due to its low r-WGS activity, while the catalysts containing no chlorine component show quite low CO/CO_2 selectivity.
- The evaluation of the activity of the Ni/TiO_2 catalysts prepared from Ni salt solutions with different mixing molar ratios of Ni chloride to Ni nitrate proved that a trace amount of chlorine resulted in the improved CO/CO_2 reaction selectivity in CO-SMET. The chlorine component in the Ni/TiO_2 catalysts is considered to be located on the interface of the Ni particles and the TiO_2 support, giving rise to the suppression of CO_2 methanation via the r-WGS step.

Acknowledgment

This work was supported by the New Energy and Industrial Technology Development Organization (NEDO, Japan, Grant 08002078-0 and 100000858-0). TEM analysis was supported by the Cooperative Research Program of Catalysis Research Center, Hokkaido University (Grant 14B1009).

References

[1] V. Recupero, L. Pino, M. Cordaro, A. Vita, F. Cipitì, M. Laganà, Fuel Process. Technol. 85 (2004) 1445–1452.
[2] C. Pedrero, T. Waku, E. Iglesia, J. Catal. 233 (2005) 242–255.
[3] I. López, T. Valdés-Solís, G. Marbán, Int. J. Hydrogen Energy 33 (2008) 197–205.
[4] O. Pozdnyakova, D. Teschner, A. Wootsch, J. Kröhnert, B. Steinhauer, H. Sauer, L. Toth, F.C. Jentoft, A. Knop-Gericke, Z. Paál, R. Schlögl, J. Catal. 237 (2006) 1–16.
[5] S.H. Oh, R.M. Sinkevitch, J. Catal. 142 (1993) 254–262.
[6] R.M.T. Sanchez, A. Ueda, K. Tanaka, M. Haruta, J. Catal. 168 (1997) 125–127.
[7] G. Sedmak, S. Hočevar, J. Levec, J. Catal. 213 (2003) 135–150.
[8] D. Gamarra, A. Martínez-Arias, J. Catal. 263 (2009) 189–195.
[9] E.D. Park, D. Lee, H.C. Lee, Catal. Today 139 (2009) 280–290.
[10] P. Djinović, C. Galletti, S. Specchia, V. Specchia, Catal. Today 164 (2011) 282–287.
[11] C. Galletti, S. Specchia, V. Specchia, Chem. Eng. J. 167 (2011) 616–621.
[12] P. Panagiotopoulou, D.I. Kondarides, X.E. Verykios, Appl. Catal. A: Gen. 344 (2008) 45–54.
[13] Z. Kowalczyk, K. Stołecki, W. Raróg-Pilecka, E. Miśkiewicz, E. Wilczkowska, Z. Karpiński, Appl. Catal. A: Gen. 342 (2008) 35–39.
[14] R.A. Dagle, Y. Wang, G.G. Xia, J.J. Strohm, J. Holladay, D.R. Palo, Appl. Catal. A: Gen. 326 (2007) 213–218.
[15] M. Echigo, T. Tabata, J. Chem. Eng. Jpn. 37 (2004) 75–81.
[16] Z.G. Zhang, G. Xu, Catal. Commun. 8 (2007) 1953–1956.
[17] S. Eckle, M. Augustin, H.G. Anfang, R.J. Behm, Catal. Today 181 (2012) 40–51.
[18] S. Eckle, H.G. Anfang, R.J. Behm, Appl. Catal. A: Gen. 391 (2011) 325–333.
[19] S. Eckle, Y. Denkwitz, R.J. Behm, J. Catal. 269 (2010) 255–268.
[20] A.M. Abdel-Mageed, S. Eckle, R.J. Behm, J. Catal. 208 (2013) 148–160.
[21] M. Kimura, T. Miyao, S. Komori, A. Chen, K. Higashiyama, H. Yamashita, M. Watanabe, Appl. Catal. A: Gen. 379 (2010) 182–187.
[22] T. Miyao, W. Shen, A. Chen, K. Higashiyama, M. Watanabe, Appl. Catal. A: Gen. 486 (2014) 187–192.
[23] A. Chen, T. Miyao, K. Higashihara, H. Yamashita, M. Watanabe, Angew. Chem. Int. Ed. 49 (2010) 9895–9898.
[24] P. Panagiotopoulou, D.I. Kondarides, X.E. Verykios, Catal. Today 181 (2012) 138–147.
[25] P. Panagiotopoulou, D.I. Kondarides, X.E. Verykios, Appl. Catal. B: Environ. 88 (2009) 470–478.
[26] S. Takenaka, T. Shimizu, K. Otsuka, Int. J. Hydrogen Energy 29 (2004) 1065–1073.
[27] Y. Wang, R. Wu, Y. Zhao, Catal. Today 158 (2010) 470–474.
[28] Q. Liu, X. Dong, X. Mo, W. Lin, J. Nat. Gas Chem. 17 (2008) 268–272.
[29] Y. Men, G. Kolb, R. Zapf, V. Hessel, H. Löwe, Catal. Today 125 (2007) 81–87.
[30] M.R. Prairie, A. Renken, J.G. Highfield, K.R. Thampi, M. Grätzel, J. Catal. 129 (1991) 130–144.
[31] F. Solymosi, A. Erdöhelyi, J. Mol. Catal. 8 (1980) 471–474.
[32] G.D. Weatherbee, C.H. Bartholomew, J. Catal. 87 (1984) 352–362.
[33] J.M. Rynkowski, T. Paryjczak, A. Lewicki, M.I. Szynkowska, T.P. Maniecki, W.K. Jóźwiak, React. Kinet. Catal. Lett. 71 (2000) 55–64.
[34] M. Marwood, F. van Vyve, R. Doepper, A. Renken, Catal. Today 20 (1994) 437–448.
[35] M. Marwood, R. Doepper, A. Renken, Appl. Catal. A: Gen. 151 (1997) 223–246.
[36] N.M. Gupta, V.S. Kamble, V.B. Kartha, R.M. Iyer, K. Ravindranathan Thampi, M. Grazel, J. Catal. 146 (1994) 173–184.
[37] S. Mori, W.C. Xu, T. Ishidzuki, N. Ogasawara, J. Imai, K. Kobayashi, Appl. Catal. A: Gen. 137 (1996) 255–268.
[38] F. Solymosi, A. Erdöhelyi, M. Kocsis, J. Chem. Soc. Faraday Trans. 1 77 (1981) 1003–1012.
[39] C. de Leitenburg, A. Trovarelli, J. Kaspar, J. Catal. 166 (1997) 98–107.
[40] S. Tada, O.J. Ochieng, R. Kikuchi, T. Haneda, H. Kameyama, Int. J. Hydrogen Energy 39 (2014) 10090–10100.
[41] F. Solymosi, A. Erdöhelyi, T. Bánsági, J. Catal. 68 (1981) 371–382.
[42] M.A. Henderson, S.D. Worley, J. Phys. Chem. 89 (1985) 1417–1423.
[43] W.H. Weinberg, Surf. Sci. 128 (1983) L224–L230.
[44] L.H. Dubois, G.A. Somorjai, Surf. Sci. 128 (1983) L231–L235.
[45] D.W. Goodman, D.E. Peebles, J.M. White, Surf. Sci. 140 (1984) L239–L243.
[46] F. Solymosi, J. Kiss, Chem. Phys. Lett. 110 (1984) 639–642.
[47] M. Bowker, T.J. Cassidy, A.T. Ashcroft, A.K. Cheetham, J. Catal. 143 (1993) 308–313.
[48] F. Solymosi, A. Erdöhelyi, T. Bánsági, J. Chem. Soc. Faraday Trans. 1 77 (1981) 2645–2657.
[49] A. Erdöhelyi, M. Pásztor, F. Solymosi, J. Catal. 98 (1986) 166–177.
[50] J.-N. Park, E.W. McFarland, J. Catal. 266 (2009) 92–97.
[51] H. Song, J. Yang, J. Zhao, L. Chou, Chin. J. Catal. 31 (2010) 21–23.
[52] E. Vesselli, L. de Rogatis, X. Ding, A. Baraldi, L. Savio, L. Vattuone, M. Rocca, P. Fornasiero, M. Peressi, A. Baldereschi, R. Rosei, G. Comelli, J. Am. Chem. Soc. 130 (2008) 11417–11422.
[53] A.E. Aksoylu, A.N. Akın, Z.İ. Önsan, D.L. Trimm, Appl. Catal. A: Gen. 145 (1996) 185–193.
[54] G.M. Shashidhara, M. Ravindram, React. Kinet. Catal. Lett. 37 (1988) 451–456.
[55] S. Furukawa, M. Okada, Y. Suzuki, Energy Fuels 13 (1999) 1074–1081.
[56] M. Yamasaki, H. Habazaki, K. Asami, K. Izumiya, K. Hashimoto, Catal. Commun. 7 (2006) 24–28.
[57] H. Habazaki, M. Yamasaki, A. Kawashima, K. Hashimoto, Appl. Organomet. Chem. 14 (2000) 803–808.
[58] S. Tada, T. Shimizu, H. Kameyama, T. Haneda, R. Kikuchi, Int. J. Hydrogen Energy 37 (2012) 5527–5531.
[59] M. Tsuji, T. Kodama, T. Yoshida, Y. Kitayama, Y. Tamaura, J. Catal. 164 (1996) 315–321.

[60] J. Sehested, K. Larsen, A. Kustov, A. Frey, T. Johannessen, T. Bligaard, M. Andersson, J. Nørskov, C. Christensen, Top. Catal. 45 (2007) 9–13.
[61] S. Tada, R. Kikuchi, K. Urasaki, S. Satokawa, Appl. Catal. A: Gen. 404 (2011) 149–154.
[62] K. Urasaki, K. Endo, T. Takahiro, R. Kikuchi, T. Kojima, S. Satokawa, Top. Catal. 53 (2010) 707–711.
[63] K. Urasaki, Y. Tanpo, T. Takahiro, J. Christopher, R. Kikuchi, T. Kojima, S. Satokawa, Chem. Lett. 39 (2010) 972–973.
[64] K. Urasaki, Y. Tanpo, Y. Nagashima, R. Kikuchi, S. Satokawa, Appl. Catal. A: Gen. 452 (2013) 174–178.
[65] S. Tada, R. Kikuchi, A. Takagaki, T. Sugawara, S.T. Oyama, K. Urasaki, S. Satokawa, Appl. Catal. B: Environ. 140–141 (2013) 258–264.
[66] S. Tada, R. Kikuchi, A. Takagaki, T. Sugawara, S.T. Oyama, S. Satokawa, Catal. Today 232 (2014) 16–21.
[67] S. Tada, D. Minori, F. Otsuka, R. Kikuchi, K. Osada, K. Akiyama, S. Satokawa, Fuel 129 (2014) 219–224.
[68] S. Tada, R. Kikuchi, K. Wada, K. Osada, K. Akiyama, S. Satokawa, Y. Kawashima, J. Power Source 264 (2014) 59–66.
[69] P. Djinovic, C. Galletti, S. Specchia, V. Specchia, Top. Catal. 54 (2011) 1042–1053.
[70] M.M. Zyryaniva, P.V. Snytnikov, R.V. Gulyaev, Y.I. Amosov, A.I. Boronin, V.A. Sobyanin, Chem. Eng. J. 238 (2014) 189–197.